

## Redistribution of an Intergranular-Liquid Phase During Sintering of 1 mol%-Al<sub>2</sub>O<sub>3</sub>-doped Calcia-Stabilized Zirconia: Estimation by Impedance Spectroscopy

Jung-Hae Choi, Jong-Heun Lee<sup>†</sup> and Doh-Yeon Kim

*School of Materials Science and Engineering and Center for Microstructure Science of Materials,  
Seoul National University, Seoul 151-744, Korea*

(Received September 4, 2002; Accepted September 18, 2002)

### ABSTRACT

The grain boundary resistivity of a 1-mol%-Al<sub>2</sub>O<sub>3</sub>-doped CaO-Stabilized Zirconia(CSZ) specimen was determined by impedance spectroscopy using sub-millimeter-scale electrodes. At the initial stage of sintering, the grain-boundary resistivity of the specimen interior was observed to be higher than that of the surface. However, upon further sintering the boundary resistivity of the specimen interior became lower than that of the surface. The results were explained in terms of a redistribution of the intergranular liquid phase. The liquid phase was predicted to initially coagulate at the interior of the specimen then spread outward during sintering.

**Key words :** Al<sub>2</sub>O<sub>3</sub>-doped CSZ, Sintering, Redistribution of liquid phase, Impedance spectroscopy, Grain boundary resistivity

### 1. Introduction

Recently, the grain-boundary resistivity of 1 mol%-Al<sub>2</sub>O<sub>3</sub>-doped 15 mol% CaO-stabilized zirconia (denoted as 15CSZ-1A) specimen has been reported to vary substantially from the surface to the interior. This phenomenon was explained by different local characteristics of the intergranular liquid.<sup>1)</sup> At the near-surface region of the sintered specimen, most of the grain boundaries were penetrated by the liquid with a low dihedral angle ( $\phi = \sim 20^\circ$ ). In contrast, the liquid phase at the specimen interior showed a high dihedral angle ( $\phi = \sim 100^\circ$ ). As a result, the boundary resistivity of the specimen surface was much higher than that of the specimen interior. From the compositional difference between two liquids, a possible phase separation of the liquid was suggested. However, it is uncertain how the liquids of low and high  $\phi$  are concentrated at the specimen surface and interior, respectively.

Indeed, during sintering in the presence of a liquid-phase, it has been well established<sup>2)</sup> that the liquid can flow freely and assume the configurations of the lowest interface energy. When mixtures of W and 1 wt% of Ni powders are sintered, liquid Ni is observed to agglomerate initially at the specimen center to decrease the total liquid-vapor interface area then spread outward upon further sintering.<sup>3)</sup> The agglomeration of a very small amount of TiO<sub>2</sub>-enriched liq-

uid into the interior of BaTiO<sub>3</sub> specimens has also been observed.<sup>4)</sup> In this respect, the process of liquid flow and its redistribution are also expected to occur during the sintering of 15CSZ-1A specimens. Therefore, the variation in grain boundary resistivity would be a consequence of such liquid redistribution.

On the other hand, grain boundary contribution in the impedance spectroscopy has been well known to be very sensitive to the microstructure and configuration of the intergranular liquid.<sup>5-8)</sup> But the conventional impedance spectroscopy based on the brick layer model cannot estimate the local inhomogeneity of grain boundaries. Recently impedance spectroscopy with sub-millimeter-scale electrodes was developed and successfully used to investigate the distribution of a highly resistive intergranular phase.<sup>1)</sup>

The purpose of this study was to experimentally determine whether or not liquid redistribution occurs during the sintering of a 15CSZ-1A specimen. The main focus of this investigation was to understand why a liquid with a low dihedral angle is located at the specimen surface.

### 2. Experimental

15 mol% Calcia Stabilized Zirconia(CSZ) powder (CSZ-15 Heat-treated, Daiichi Kigenso Kagaku Kogyo Co. Ltd., Osaka, Japan) was used as a raw material. The impurity concentrations of SiO<sub>2</sub>, TiO<sub>2</sub>, FeO<sub>3</sub> and Na<sub>2</sub>O were 0.04, 0.09, 0.026 and 0.02 wt%, respectively. With the addition of 1 mol% of Al<sub>2</sub>O<sub>3</sub> (AKP3000, Sumitomo Chemical Co., Tokyo, Japan), the powder mixture was ball-milled for 6 h in ethyl alcohol using partially stabilized zirconia balls. After dry-

<sup>†</sup>Corresponding author : Jong-Heun Lee

E-mail : jongheun@gong.snu.ac.kr

Tel : +82-2-880-6891 Fax : +82-2-884-1413

ing, 7 g of the powder was uniaxially pressed into a cylindrical rod shaped specimen then isostatically pressed at 200 MPa. The compacts were sintered for 4 h in air at two different sintering temperatures; 1550 and 1450°C. The heating rate was 200°C/h.

A slab of 11×13×0.55 mm<sup>3</sup> was obtained by cutting along the diameter of the cylinder-shape specimen (diameter: 11 mm, height: 13 mm). On each side of the slab, 6 electrodes were made from the surface to the center along the longer direction with a 0.5 mm spacing by screen-printing a Pt paste (TR 7905, Tanaka Co., Tokyo, Japan). The size of each rectangular electrode was 2×0.5 mm<sup>2</sup>. After drying, the specimen was heat-treated at 1100°C for 1 h. The electrodes were mechanically contacted with S-type thermocouples to measure the temperature and local impedance concurrently. For these measurements, an AC two-probe technique by SI 1260 impedance/gain-phase analyzer (Model No. SI 1260, Solartron, Inc., Farnborough, U.K.) was used. The detailed electrode configuration and experimental setup was illustrated in the previous report.<sup>11</sup> The data was obtained at 400°C in air. The average grain size of the specimens was determined by multiplying 1.775 to the mean intercept length.<sup>9)</sup>

### 3. Results and Discussions

Fig. 1 shows the microstructure of a typical specimen obtained after the sintering for 4 h at 1550°C. The specimen has a uniform microstructure throughout and little variation in grain size from the surface to the interior. Although the dark phases (indicated by arrows) were identified as the intergranular phase containing CaO, SiO<sub>2</sub>, Al<sub>2</sub>O<sub>3</sub> and ZrO<sub>2</sub> and observed both at the specimen surface and at the interior, the characteristics, such as a difference in wettability could not be clearly discerned by the conventional SEM (Scanning Electron Microscopy). The average grain size was determined to be 25.5 μm. The microstructure of the specimen obtained after the sintering at 1450°C was quite simi-



Fig. 1. The microstructure of the specimen sintered at 1550°C for 4 h.

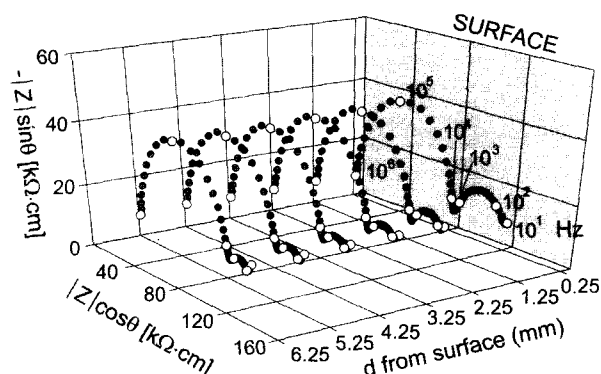


Fig. 2. Complex impedance spectra of the specimen sintered at 1550°C for 4 h as a function of distance from the surface (measured at 400°C in air).

lar to that shown in Fig. 1 except for the smaller average grain size (9.7 μm).

Fig. 2 shows the variation in the complex impedance spectra as a function of the distance from the surface,  $d$ , of the specimen shown in Fig. 1. The three contributions from the low frequencies are those from the electrode polarization, grain boundary and grain interior, respectively. It should be noted that the apparent grain-boundary resistivity ( $\rho_{gb}$ ) deconvoluted from the impedance spectrum varied to a large extent with a distance from the surface, while the grain-interior resistivity ( $\rho_{gi}$ ) remained almost constant at 82 kΩ·cm.

From the  $\rho_{gb}$  value obtained, the resistance per unit grain boundary area ( $R_{gbs}$ ) can be calculated from the following equation:<sup>10)</sup>

$$R_{gbs} = \rho_{gb} / D \quad (1)$$

where  $D$  is the grain-boundary density (number of grain boundary per unit length) that is the reciprocal of the average grain size ( $d_g$ ). The  $R_{gbs}$  values determined from the specimens are shown in Fig. 3. As this figure shows, the  $R_{gbs}$  values of the specimen sintered at 1550°C decreased with increasing  $d$  then became approximately constant when  $d$  exceeded 3 mm. The results suggest that the grain boundary at the surface is approximately 2.5 times more resistive compared to that at the center.

In a previous study,<sup>11</sup> it was reported that the grain boundary at the surface is ~15 times more resistive than that at the center for a specimen sintered at 1650°C. TEM (Transmission Electron Microscopy) observations showed that the average dihedral angle of the liquid was ~20° at the surface and ~100° at the interior. In fact, Souza *et al.*<sup>11)</sup> suggested that a phase separation of the liquid glass occurs and the phase-separated glass is expelled outward during the liquid-phase sintering of yttria-stabilized zirconia. Note this suggestion implies that the liquid coagulates at the initial stage of sintering.

In order to examine the above possibility, the specimen was sintered at 1450°C for 0 h and then furnace-cooled. Sin-

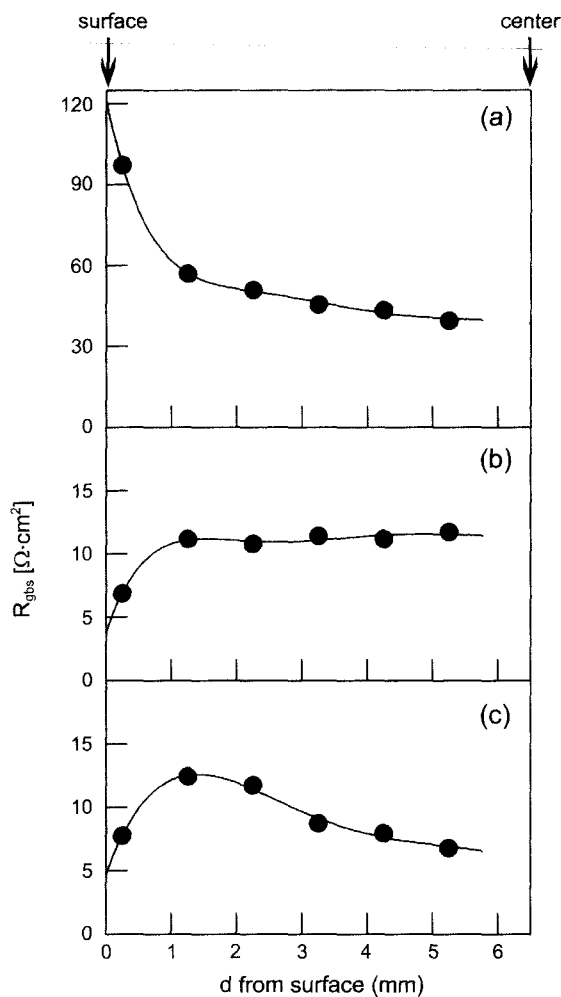


**Fig. 3.** The profile of the resistance per unit grain-boundary area ( $R_{\text{gbs}}$ ) for the specimens sintered at (a) 1550°C for 4 h, (b) 1450°C for 0 h and (c) and 1450°C for 4 h. (measured at 400°C in air).

tering for 0 h means that the specimen was cooled immediately after the sintering temperature reached. In this case, the average grain size was found to be 3.0  $\mu\text{m}$ . As shown in Fig. 3(b), this specimen exhibited a lower boundary resistivity at the surface compared to that of the interior. The  $R_{\text{gbs}}$  values at the surface ( $d=0.25$  mm) and at the interior ( $d>0.5$  mm) were 6.9 and  $11.3\pm 0.3$   $\Omega\cdot\text{cm}^2$ , respectively. This is most likely a consequence of the intergranular liquid that coagulated at the interior of the specimen. Note also that the  $R_{\text{gbs}}$  values shown in Fig. 3(a) are substantially higher than those shown in Fig. 3(b), which can be attributed to the increase in thickness of the resistive intergranular liquid phase with grain growth.

On the other hand, Fig. 3(c) shows a variation in the boundary resistivity obtained from the specimen sintered at 1450°C for 4 h and then cooled at a rate of 200°C/h. In this case, the  $R_{\text{gbs}}$  value at the surface was still quite low but showed a maximum at  $d=1.25$  mm, then gradually decreased with further increases in  $d$ . The change from Fig. 3(b)

to (c) is expected to be the consequence of the outward flow of the coagulated liquid. In liquid-phase sintering, the coagulated liquid is observed to flow outward as densification proceeds.<sup>2)</sup> The specimen densities after sintering at 1450°C for 0 h and 4 h were 5.28 and 5.41  $\text{g}/\text{cm}^3$ , respectively. The specimen that was furnace-cooled after sintering at 1450°C for 4 h showed a similar  $\rho_{\text{gb}}$  profile, indicating that the outward flow is not related with the cooling schedule.

The process of liquid rearrangement during liquid-phase sintering is known to critically depend on the wetting characteristic and viscosity of the liquid, the grain size and the pore capillary size.<sup>2,12,13)</sup> However, liquid phase separation should be taken into account on sintering a 15CSZ-1A specimen. During the infiltration process, the height of liquid rise ( $H$ ) can be described by the following equation:<sup>14)</sup>

$$H = \frac{2\gamma_{\text{LV}}\cos\theta}{D_{\text{L}}gR_{\text{C}}} \quad (2)$$

where  $\gamma_{\text{LV}}$ ,  $\theta$ ,  $D_{\text{L}}$ ,  $g$ ,  $R_{\text{C}}$  are the liquid-vapor surface energy, the contact angle, the liquid density, gravity and the radius of the capillary, respectively. Considering that  $\phi$  is usually proportional to  $\theta$ , the lower the  $\phi$ , the higher the  $H$  value predicted. This indicates that, when phase separation of a coagulated liquid occurs, the liquid with low  $\phi$  would preferentially flow outward. The high boundary resistivity of the 15CSZ-1A specimen surface is therefore the result of liquid outward flow during sintering.

#### 4. Conclusion

During the sintering of a 1-mol%- $\text{Al}_2\text{O}_3$ -doped 15 mol% CSZ specimen, an intergranular liquid was observed to coagulate in the initial stages of sintering then flowed outward as densification progressed. Due to liquid phase separation, however, the liquid flowing outward was mainly that of a low dihedral angle. As a result, the grain boundary resistivity of the specimen surface became much higher than that of the interior. Impedance spectroscopy is useful for predicting the rearrangement of the intergranular liquid phase that is difficult to observe through conventional microscopy.

#### Acknowledgment

This work was supported by the Center for Iron and Steel Research at Seoul National University.

#### REFERENCES

1. J.-H. Lee, J. H. Lee and D.-Y. Kim, "The Inhomogeneity of Grain-boundary Resistivity in Calcia-stabilized Zirconia," *J. Am. Ceram. Soc.*, **85** [6] 1622-24 (2002).
2. T. M. Shaw, "Liquid Redistribution during Liquid-phase Sintering," *J. Am. Ceram. Soc.*, **69** [1] 27-34 (1986).
3. O.-J. Kwon and D. N. Yoon, "The Liquid Phase Sintering of W-Ni," in *Sintering and Related Phenomena*, edited by G.

- C. Kuczynski, Plenum Publishing Company, pp.203-218, 1980.
4. Y.-S. Yoo, J.-J. Kim and D.-Y. Kim, "Effect of Heating Rate on the Microstructural Evolution During Sintering of BaTiO<sub>3</sub> Ceramics," *J. Am. Ceram. Soc.*, **70** [11] C322-24 (1987).
  5. J.-W. Moon, G.-D. Kim, K.-T. Lee and H.-L. Lee, "Effect of YSZ Particle Size and Sintering Temperature on the Microstructure and Impedance Property of Ni-YSZ Anode for Solid Oxide Fuel Cell," *J. Kor. Ceram. Soc.*, **38** [5] 466-73 (2001).
  6. J.-H. Lee and S.-H. Cho, "Effect of Abnormal Grain Growth and Heat Treatment on Electrical Properties of Semiconducting BaTiO<sub>3</sub> Ceramics," *J. Kor. Ceram. Soc.*, **39** [1] 21-5 (2002).
  7. S. J. Kim, K. H. Kim, S. J. Oh, T. K. Kang and I. H. Kuk, "Effect of Microstructural Design on the Electrical Properties of Y<sub>2</sub>O<sub>3</sub>-stabilized ZrO<sub>2</sub>," *J. Kor. Ceram. Soc.*, **30** [9] 717-22 (1993).
  8. J.-H. Lee, T. Mori, J.-G. Li, T. Ikegami and S. Takenouchi, "Impedance Spectroscopic Estimation of Inter-granular Phase Distribution in 15 mol% Calcia-stabilized Zirconia/Alumina Composites," *J. Euro. Ceram. Soc.*, **21** [1] 13-7 (2001).
  9. J.-H. Han and D.-Y. Kim, "Analysis of the Proportionality Constant Correlating the Mean Intercept Length to the Average Grain Size," *Acta Metall. Mater.*, **43** [8] 3183-88 (1995).
  10. M. Miyayama, H. Yanagida and A. Asada, "Effect of Al<sub>2</sub>O<sub>3</sub> Addition on Resistivity and Microstructure of Yttria-stabilized Zirconia," *Am. Ceram. Soc. Bull.*, **65** [4] 660-64 (1986).
  11. D. P. E. De Souza and M. F. De. Souza, "Liquid Phase Sintering of Re<sub>2</sub>O<sub>3</sub>: YSZ Ceramics" Part I Grain Growth and Expelling of the Grain Boundary Glass Phase," *J. Mater. Sci.*, **34** 4023-30 (1999).
  12. H.-H. Park, S.-J. Cho and D.-N. Yoon, "Pore Filling Process in Liquid Phase Sintering," *Metall. Trans. A*, **15A** 1075-80 (1984).
  13. O.-J. Kwon and D. N. Yoon, "Closure of Isolated Pores in Liquid Phase Sintering of W-Ni," *Int. J. Powder Metall.*, **17** [2] 127-33 (1981).
  14. J. S. Reed, Principles of Ceramic Processing, A Wiley-Interscience Publication, p.25 (1995).